Published in final edited form as:
Biochemistry. 2008 October 28; 47(43): 11340–11347. doi:10.1021/bi801503r.

Conformational Flexibility of the N-terminal Domain of Apolipoprotein A-I Bound to Spherical Lipid Particles

Momoe Kono[‖], **Yusuke Okumura**[‖], **Masafumi Tanaka**[‖], **David Nguyen**[‡], **Padmaja Dhanasekaran**[‡], **Sissel Lund-Katz**[‡], **Michael C. Phillips**[‡], and **Hiroyuki Saito**[‖,*]

‖*Department of Biophysical Chemistry, Kobe Pharmaceutical University, Kobe 658-8558, Japan*

‡*Division of GI/Nutrition/Hepatology, The Children's Hospital of Philadelphia, University of Pennsylvania School of Medicine, Philadelphia, Pennsylvania 19104-4318*

Abstract

Lipid binding of human apolipoprotein A-I (apoA-I) occurs initially through the C-terminal α-helices followed by conformational reorganization of the N-terminal helix bundle. This led us to hypothesize that apoA-I has multiple lipid-bound conformations, in which the N-terminal helix bundle adopts either open or closed conformations anchored by the C-terminal domain. To investigate such possible conformations of apoA-I at the surface of a spherical lipid particle, site-specific labeling of the N- and C-terminal helices in apoA-I by *N*-(1-pyrene)maleimide was employed after substitution of a Cys residue for Val-53 or Phe-229. Neither mutagenesis nor the pyrene labeling caused discernible changes in the lipid-free structure and lipid interaction of apoA-I. Taking advantage of a significant increase in fluorescence when a pyrene-labeled helix is in contact with the lipid surface, we monitored the behaviors of the N- and C-terminal helices upon binding of apoA-I to egg PC small unilamellar vesicles. Comparison of the binding isotherms for pyrene-labeled apoA-I as well as a C-terminal helical peptide suggests that an increase in surface concentration of apoA-I causes dissociation of the N-terminal helix from the surface leaving the C-terminal helix attached. Consistent with this, isothermal titration calorimetry measurements showed that the enthalpy of apoA-I binding to the lipid surface under near saturated conditions is much less exothermic than that for binding at a low surface concentration, indicating the N-terminal helix bundle is out of contact with lipid at high apoA-I surface concentrations. Interestingly, the presence of cholesterol significantly induces the open conformation of the helix bundle. These results provide insight into the multiple lipid-bound conformations that the N-terminal helix bundle of apoA-I can adopt on a lipid or lipoprotein particle, depending upon the availability of space on the surface and the surface composition.

High density lipoprotein (HDL) is of great clinical importance because elevated levels of plasma HDL cholesterol are associated with a reduced incidence of coronary artery disease (1,2). Apolipoprotein A-I (apoA-I) is the principal protein in HDL and it plays a central role in HDL metabolism (3). The protective functions of HDL and apoA-I against coronary artery disease are due in part to their participation in reverse cholesterol transport, a process by which cholesterol in peripheral cells is transferred via HDL to the liver for catabolism (4,5). The ability of apoA-I to bind to lipid membranes, receptors, and ATP-binding cassette (ABC) transporters at cell surfaces is central to mediating the transport of cholesterol into and out of cells (6-8).

*To whom correspondence should be addressed: Dr. Hiroyuki Saito Department of Biophysical Chemistry Kobe Pharmaceutical University 4-19-1 Motoyamakitamachi Kobe 658-8558, Japan Tel: +81-78-441-7539 Fax: +81-78-441-7541 E-mail: saito@kobepharma-u.ac.jp.

ApoA-I is a 243-residue polypeptide that contains characteristic 11- and 22-residue repeats of amphipathic α-helices (9). The N- and C-terminal helical regions in the apoA-I molecule contribute to the strong lipid binding properties of this protein (10-12) as well as the conformational stability in solution (13,14). It has been demonstrated recently that the apoA-I molecule folds into two tertiary structure domains, comprising an N-terminal α-helix bundle spanning residues 1-187 and a separate less organized C-terminal region spanning the remainder of the molecule (15-17). The links between this two-domain structure and the function of apoA-I remain to be elucidated (18,19).

HDL particles are quite heterogeneous in size and composition (20). In discoidal HDL particles, it is well known that the apoA-I molecules are organized into a belt-like arrangement around the edge of discoidal particles (21-23). Recent reports using site-directed spin label electron paramagnetic resonance (24) and hydrogen-deuterium exchange mass spectroscopy (25) suggested that a central region of apoA-I bound to discoidal HDL particles forms a protruding solvent-exposed looped conformation, although such an organization seems to be energetically unfavorable (26). In soluble apolipoproteins such as apoA-I and apoE consisting of a number of different amphipathic helices, the conformational flexibility of the proteins could allow some helices with low lipid affinity to be excluded from the particle surface (9,18,27,28). Indeed, we demonstrated previously that the two domain structure in apoE leads to two different lipid-bound conformations on lipoprotein-like spherical particles; the N-terminal four-helix bundle can adopt either open or closed conformations, resulting from binding competition with the C-terminal domain that has a high lipid affinity (29). Given the similar domain structure of apoA-I and apoE (15,18), it is conceivable that the apoA-I molecules on lipoprotein particles have also multiple lipid-bound conformations to adapt to changes in surface availability during remodeling of lipoprotein particles (28,30,31). Previous studies suggested that the apoA-I in spherical HDL is flexible with its conformation being governed by the size and core lipid composition of the particles (32,33). However, little is known about the organization of the apoA-I molecules on spherical HDL particles to date (34).

In the current study, we examined the lipid-bound conformations of apoA-I on spherical lipid particles by employing site-directed fluorescence labeling of apoA-I. To monitor the lipid binding behaviors of the N- and C-terminal domains, a cysteine residue was introduced into the N- and C-terminal helical segments, amino acids 44-65 and 220-241 that possess the strongest lipid affinity among putative amphipathic α-helices in the apoA-I molecule (10), for attachment of the extrinsic fluorescence probe pyrene (35-38). The results suggest that apoA-I has at least two lipid-bound conformations in which the N-terminal helix bundle is either open or closed, depending upon the availability of the lipid surface. In addition, effects of cholesterol on the equilibrium between such two lipid-bound conformations of apoA-I are examined.

EXPERIMENTAL PROCEDURES

Proteins and Peptide

The mutations in apoA-I to introduce cysteine residue into Val-53 or Phe-229 were made using the QuikChange site-directed mutagenesis kit (Stratagene, La Jolla, CA). Wild type (WT) apoA-I and engineered mutants were expressed and purified as described (15,19). The apoA-I preparations were at least 95 % pure as assessed by SDS-PAGE. The C-terminal apoA-I (220-241/F229C) peptide was synthesized at Sigma Genosys (Hokkaido, Japan) with an acetylated N-terminus and an amidated C-terminus. Peptide purity was verified by analytical HPLC (>97%) and mass spectrometry. In all experiments, apoA-I variants and peptide were freshly dialyzed from 6 M guanidine hydrochloride (GdnHCl) and 1% β-mercaptoethanol solution into the appropriate buffer before use.

Site-specific Pyrene Labeling

Cysteine-containing apoA-I variants or peptide were incubated with 10-fold molar excess of tris(2-carboxyethyl)phosphine hydrochloride (Pierce, Rockford, IL) for 1 h to reduce the sulfhydryl group. The 10 mM stock solution of *N*-(1-pyrene)maleimide (Molecular Probes, Inc., Eugene, OR) in DMSO was added so that a final molar ratio of probe to protein was 10:1 (or 3:1 for peptide). The reaction mixtures were then stirred at room temperature for 3 h in the dark. Unreacted *N*-(1-pyrene)maleimide was removed by extensive dialysis at 4 °C in Tris buffer (10 mM Tris, 150 mM NaCl, 1 mM EDTA, 0.02 % NaN_3, pH 7.4). The degree of labeling was determined using the extinction coefficient for pyrene of 38,200 M^{-1} cm^{-1} at 338 nm and found to range from 60 to 100 %.

Preparation of SUV

Small unilamellar vesicles (SUVs) were prepared as described (11,14). Briefly, a film of egg phosphatidylcholine (PC) with or without cholesterol on the wall of a glass tube was dried under vacuum overnight. The lipid was then hydrated in Tris buffer and sonicated on ice under nitrogen. After removing titanium debris, the samples were centrifuged in a Beckman TLA110 rotor for 2 h at 4 °C at 51,000 rpm to separate any remaining large vesicles. The PC and cholesterol concentrations of SUV were determined using enzymatic assay kits from Wako Pure Chemicals (Osaka, Japan).

Circular Dichroism (CD) Spectroscopy

Far-UV CD spectra were recorded from 185 to 260 nm at 25 °C using an Aviv 62DS spectropolarimeter. After dialysis from 6M GdnHCl solution, the apoA-I sample was diluted to 25-50 μg/ml in 10 mM sodium phosphate buffer (pH 7.4) and the CD spectrum was obtained. For the apoA-I-SUV mixture sample, apoA-I was incubated with SUV for 1 h prior to the measurement. The results were corrected by subtracting the buffer baseline or a blank sample containing an identical concentration of SUV. The α-helix content was calculated from the molar ellipticity at 222 nm, as described (39). For monitoring chemical denaturation, proteins at a concentration of 50 μg/ml were incubated overnight at 4 °C with GdnHCl at various concentrations. K_D at a given GdnHCl concentration was calculated from the ellipticity values and, the free energy of denaturation, $\Delta G_D°$, the midpoint of denaturation, $D_{1/2}$, and m value which reflects the cooperativity of denaturation in the transition region, were determined by the linear equation, $\Delta G_D = \Delta G_D° - m[\text{GdnHCl}]$, where $\Delta G_D = - RT \ln K_D$ (14,39).

Fluorescence Measurements

Fluorescence measurements were carried out with a Hitachi F-7000 fluorescence spectrophotometer at 25 °C in Tris buffer (pH 7.4). In SUV binding experiments, pyrene emission fluorescence of proteins or peptide (15-25 μg/ml) was recorded from 360 to 500 nm using a 342 nm excitation wavelength at increasing concentrations of SUV (ratios of PC to protein or peptide were 0-100 w/w). To reduce the effect of light scattering caused by vesicles, the sample was excited with vertically polarized light and measured with a horizontal emission polarizer using a 4 × 4 mm cuvette (40). Kinetic data for the increase in fluorescence of pyrene-labeled apoA-I variants upon SUV binding were obtained by monitoring the emission intensity at 385 nm. In quenching experiments by 5-doxylstearic acid (5-DSA), 5-DSA was incorporated into the membrane bilayer by adding aliquots of 5-DSA stock solution (13 mM in ethanol) to SUV with varying 5-DSA concentrations (35,38) before SUV was mixed with protein. For KI quenching, the pyrene emission spectra of proteins in the absence or presence of SUV were recorded at increasing concentrations of KI (0-0.56 M). After correction for dilution, the integrated fluorescence intensities were plotted according to the modified Stern-Volmer equation, $F_0/(F_0 - F) = 1/f_a + 1/f_a K_{sv}[\text{KI}]$, where F_0 and F are the fluorescence intensities in

the absence and presence of quencher, respectively, and K_{sv} and f_a are the Stern-Volmer constant and the fraction of fluorophore accessible to the quencher, respectively.

Isothermal Titration Calorimetry (ITC) Measurements

Heats of apoA-I binding to SUV were measured with a MicroCal MCS isothermal titration calorimeter at 25 °C (11,29). To measure the enthalpy of binding at a low surface concentration, apoA-I solutions were injected into SUV in the cell at a PC-to-protein molar ratio > 10,000 where the injected protein binds completely to the SUV surface. For the saturated binding condition, SUVs were injected into excess apoA-I (PC-to-protein molar ratio < 10) so that the SUV surface becomes saturated with apoA-I. Heats of dilution were determined in control experiments by injecting either apoA-I solution or SUV into buffer, and these heats were subtracted from the heats determined in the corresponding apoA-I-SUV binding experiments.

RESULTS

Effects of Mutation and Pyrene Labeling on Structure and Lipid Interaction of ApoA-I

Val-53 in the N-terminal helix (residue 44-65) or Phe-229 in the C-terminal helix (residues 220-241) were replaced with Cys because both residues are located at the middle of the nonpolar face in each helix (9). The midpoint temperatures of thermal unfolding monitored by CD were 60, 59, and 58 °C for WT, V53C, and F229C apoA-I, respectively, indicating that these Cys replacements do not cause significant structural perturbation. After labeling with pyrene, the protein structure and stability were assessed by monitoring CD. Far-UV CD spectra of V53C-pyrene and F229C-pyrene were very similar to WT (Fig. 1): the α-helix contents for WT, V53C-pyrene, and F229C-pyrene apoA-I were 46, 48, and 45%, respectively. The values of free energy of denaturation induced by GdnHCl were 3.5 ± 0.2, 3.9 ± 0.2, and 3.2 ± 0.2 kcal/mol, respectively, for WT, V53C-pyrene, and F229C-pyrene apoA-I. Furthermore, the increases in α-helix content for the apoA-I variants upon SUV binding were similar to WT (Fig. 1, *inset*). These results indicate that the pyrene labeling has little or no effect on the structure, stability and lipid interaction of apoA-I.

Pyrene Fluorescence

Binding of pyrene-labeled apoA-I to SUV was estimated using pyrene fluorescence. Fig. 2 shows typical fluorescence emission spectra of pyrene-labeled apoA-I in the absence or presence of SUV. The addition of SUV caused a large increase in fluorescence intensity of apoA-I V53C-pyrene, suggesting that the pyrene moiety is embedded in a hydrophobic environment (35,38). Consistent with this, incorporation of the lipophilic quencher 5-DSA into SUV decreased the pyrene fluorescence for both apoA-I V53C-pyrene and F229C-pyrene variants (Fig. 2, *inset*), indicating that the pyrene moiety attached to the protein is located in the lipid membrane. Furthermore, comparison of KI quenching parameters of pyrene fluorescence between the lipid-free and SUV-bound states (Table 1) showed that the f_a value for V53C-pyrene and K_{SV} value for F229C-pyrene in the SUV-bound state were lower than those in the lipid-free state, despite both the N- and C-terminal helices in apoA-I are partially masked from the aqueous phase even in the lipid-free state (41). This indicates that the pyrene moiety in the apoA-I variants becomes less exposed to the aqueous phase upon binding to SUV.

We monitored the time course of the increase in fluorescence upon binding of the pyreneapoA-I variants to SUV. As shown in Fig. 3, there was a rapid increase in pyrene fluorescence after the addition of SUV for the F229C-pyrene whereas the V53C-pyrene exhibited relatively slow kinetics. This observation is consistent with the two-step mechanism for lipid binding of apoA-I on a spherical particle: initial binding occurs rapidly through the C-terminal α-helices, followed by relatively slow conformational reorganization of the N-terminal helix bundle

(15). This indicates that the fluorescence of V53C-prene and F229C-pyrene variants is a reliable indicator for monitoring the lipid binding of the N- and C-terminal helices in apoA-I.

Fig. 4 shows the increases in fluorescence intensity of the V53C-pyrene and F229C-pyrene apoA-I variants with increasing weight ratio of PC to protein (binding titration curves). Although both variants became saturated at high PC-to-protein ratio, F229C-pyrene showed a much greater tendency to reach saturation at a lower PC-to-protein ratio compared to the V53C-pyrene variant, indicating that the pyrene molecule attached at the N- or C-terminal helices in apoA-I binds differently to the SUV surface.

Binding isotherms of apoA-I to SUV were derived from the results in Fig. 4 as follows. The fraction of bound apoA-I, θ was calculated according to

$$\theta = P_b / P_T = (F - F_0) / (F_{max} - F_0) \quad \text{(Eq. 1)}$$

where P_b and P_T are bound and total apoA-I concentrations, respectively, and F and F_0 are integrated fluorescence intensities for pyrene-apoA-I in the presence and absence of SUV, respectively, and F_{max} represents the fluorescence intensity when pyrene-apoA-I completely binds to SUV. Binding of apoA-I to lipid particles is expressed by one-site binding model assuming that apoA-I binds to discrete, equivalent, and non-interacting binding sites on the lipid particle surface (11,42-44),

$$P_b / [PC] = B_{max} P_f / (K_d + P_f) \quad \text{(Eq. 2)}$$

where P_f is unbound apoA-I concentration, [PC] is PC concentration of SUV, and K_d and B_{max} are the dissociation constant and the maximal binding capacity, respectively. Therefore, binding data can be analyzed by the Hanes-Woolf equation,

$$[PC] P_f / P_b = K_d / B_{max} + P_f / B_{max} \quad \text{(Eq. 3)}$$

Since $P_f = P_T(1-\theta)$ and $P_b = P_T\theta$, this equation is expressed as

$$[PC] (1 - \theta) / \theta = K_d / B_{max} + P_T (1 - \theta) / B_{max} \quad \text{(Eq. 4)}$$

From the linear regression lines shown in Fig. 4, *inset*, K_d and B_{max} values for pyrene-apoA-I variants were obtained (Table 2). As shown in Fig. 5, there was a good agreement between the experimental data and the theoretical binding isotherms calculated from Equation 2 and parameters shown in Table 2.

As shown in Fig. 5 and Table 2, the F229C-pyrene variant exhibited a much higher B_{max} value than that for binding of WT apoA-I to SUV determined by gel filtration experiments (11), whereas the V53C-pyrene showed a comparable value to WT. We showed previously that the two-domain structure in apoE leads to the two lipid-bound states in which the N-terminal helix bundle adopts either open or closed conformations (29,45). Given the similar domain structures of apoA-I and apoE (15,18), we assumed that apoA-I can also adopt multiple lipid-bound conformations at the SUV surface with the N-terminal helix bundle being closed and out of contact with lipid at near maximal binding. It follows that different estimations of the binding capacity will be obtained by monitoring the N- or C-terminal helices in apoA-I. To confirm this assumption, we examined the binding behavior of the C-terminal helical peptide, apoA-I (220-241/F229C)-pyrene, in which all residues are thought to be in contact with lipid on the

SUV surface. As shown in Table 2, the apoA-I (220-241/F229C)-pyrene peptide exhibited a similar B_{max} value to the value for WT apoA-I from gel filtration, indicating that the capacity of SUV binding of apoA-I in a conformation with all helices being in contact with lipid is around 0.3 amino acids/PC molecule. This suggests that the maximal binding capacity obtained for the F229C-pyrene apoA-I reflects a conformation in which most of the helices in the N-terminal domain are excluded from the lipid surface.

ITC Measurements

To confirm the notion that apoA-I has multiple lipid-bound conformations depending upon the surface concentration of protein, ITC measurements were employed. It is known that the binding of apoA-I to SUV (11,46,47) or lipid emulsions (15,42) is accompanied by a large exothermic heat. We showed previously that there was a significant difference in binding enthalpies of apoE to emulsions under the two limiting conditions of high and low surface concentration, reflecting the two lipid-bound conformations in which the N-terminal helix bundle is either open or closed (29,45). As shown in Fig. 6, binding of WT apoA-I to SUV at a low surface concentration (PC-to-protein molar ratio > 10,000) exhibited a large exothermic heat of -93 ± 5 kcal/mol protein, whereas the binding enthalpy at a saturated condition (PC-to-protein molar ratio < 10) calculated from the experimental value of -12 ± 2 cal/mol PC (Fig. 6B) using B_{max} value of 1.2 mmol apoA-I/mol PC (Table 2) was -10 ± 2 kcal/mol protein. This suggests that apoA-I binds to SUV with different conformations depending upon the surface concentration of protein. Fig. 7 compares the binding enthalpies of WT and the C-terminal domain fragment (residues 190-243) of apoA-I to SUV under the two different conditions. In contrast to WT, the binding enthalpies of apoA-I (190-243) in the two conditions were similar, suggesting that the SUV-bound conformation of apoA-I (190-243) is independent of the surface concentration of protein. Together with the results of pyrene fluorescence, ITC results suggest that at high surface concentrations of apoA-I, the N-terminal helix bundle is excluded from the lipid surface with the C-terminal domain remaining attached.

Effect of Cholesterol on the Lipid-bound Conformation of ApoA-I

Fig. 8 shows the normalized increases in fluorescence of the pyrene-apoA-I variants upon binding to egg PC/cholesterol (17/3 mol/mol) SUV. Compared to the case of egg PC SUV, the incorporation of 15 mol% of cholesterol into SUV caused much more gradual increases in fluorescence of the pyrene-apoA-I variants, especially for the F229C-pyrene, with increasing PC concentration of SUV. This indicates that the incorporation of cholesterol into SUV decreases the amount of apoA-I binding to the lipid surface (46). The difference between the binding titration curves for the V53C-pyrene and F229C-pyrene apoA-I became much smaller, suggesting that the presence of cholesterol in SUV alters the fashions in which the N- and C-terminal helices in apoA-I bind to the lipid surface. In contrast to egg PC SUV, the results of the binding titration to egg PC/cholesterol (17/3) SUV did not fit to the one-site binding model well especially in the high apoA-I concentration region. This might be because cholesterol induces multiple binding sites for apoA-I on the lipid surface such as cholesterol-poor and -rich domains (48). Therefore, we calculated the fraction of the helix bundle-closed conformation in apoA-I bound to SUV based on the notion that the fluorescence of V53C-pyrene reflects the amount of apoA-I bound with the helix bundle-open conformation whereas that of F229C-pyrene reflects the total amount of apoA-I bound to SUV. That is, the fraction of the helix bundle-closed conformation in the lipid-bound apoA-I is given as $(\theta_{F229C\text{-}pyrene} - \theta_{V53C\text{-}pyrene})/\theta_{F229C\text{-}pyrene}$. As shown in Fig. 8, *inset*, the fraction of the closed conformation for PC/cholesterol (17/3) SUV was much lower than that for PC SUV at the low PC-to-apoA-I ratio, indicating that the presence of cholesterol in SUV induces the helix bundle-open conformation in the lipid-bound apoA-I even at high surface concentrations of protein.

DISCUSSION

Previous investigation of the lipid binding properties of a series of apoA-I deletion mutants (15) led us to propose the two-step mechanism for binding of human apoA-I to a lipid surface. In this model, initial binding occurs through hydrophobic amphipathic α-helices in the C-terminal domain, followed by the slower second step in which the N-terminal helix bundle undergoes a conformational opening, converting hydrophobic helix-helix interactions to helix-lipid interactions. In agreement with this two-step process, there was a rapid increase in pyrene fluorescence upon SUV binding when the C-terminal helix was monitored, whereas there was a much slower increase for the pyrene fluorescence in the N-terminal helix (Fig. 3). Based on the reversibility of binding of apoA-I to spherical lipid particles (49-51), it is likely that dissociation of apoA-I molecules occurs in reverse: the N-terminal helix bundle dissociates from the lipid surface and closes slowly, followed by the rapid dissociation of the C-terminal domain (50). This led us to hypothesize that apoA-I has multiple lipid-bound conformations (18,28), in which the N-terminal helix bundle adopts either open or closed conformations anchored by the C-terminal domain (Fig. 9).

The results of pyrene fluorescence (Fig. 4) and ITC (Figs. 6 and 7) in this study demonstrated that apoA-I indeed has multiple conformations when bound to the SUV surface. As shown in Fig. 4, the increase in fluorescence for V53C-pyrene and F229C-pyrene apoA-I variants upon binding to egg PC SUV became saturated at a low surface concentration of protein (the PC-to-apoA-I weight ratio of ≥40), indicating that both the N- and C-terminal helices contact with lipid in that range. However, upon decreasing the PC-to-apoA-I ratio to around 10, the V53C-pyrene exhibited a gradual decrease in fluorescence while there was almost no change for the F229C-pyrene, indicating that the increase in surface concentration of apoA-I causes dissociation of the N-terminal helix from the surface leaving the C-terminal helix attached. In addition, competitive binding experiments showing that addition of unlabeled WT apoA-I to the pyrene-apoA-I variants bound to SUV at a low surface concentration caused a great decrease in fluorescence for the V53C-pyrene but negligible effects on the F229C-pyrene fluorescence (data not shown), further support the idea of multiple lipid-bound conformations of apoA-I depending upon the surface concentration of protein. In agreement with this, the favorable enthalpy of binding of apoA-I in a saturated condition where apoA-I is expected to bind to lipids only by the C-terminal domain was much lower than that at a low surface concentration where both the N- and C-terminal domains bind to lipids (Figs. 6 and 7) despite both the N- and C-terminal domains contribute to the favorable enthalpy of binding by the lipid binding-induced α-helix formation of apoA-I (11).

The conformational plasticity and molten globule characteristics of apoA-I (52) suggest a flexible and adaptable lipid-bound conformation, in which certain parts of protein with low lipid affinities are excluded from the lipid surface (18,27,28,53). The existence of a central region loosely bound to lipids in lipoprotein-bound apoA-I, called the hinge region, has been suggested (9,54) because this region consists of α-helices that have low lipid affinity (10). Indeed, it has been shown recently that a central region of apoA-I bound to discoidal HDL particles forms a protruding solvent-exposed looped conformation (24,25) although there is still some debate about which residues are out of contact with lipid (26). Similarly, it appears that apoA-I also has a flexible conformation on spherical lipid particles depending upon the availability of the lipid surface: for instance, some of the middle parts of the protein dissociate from the surface leaving the rest of the molecule attached (28) or the N-terminal may dissociate first while the C-terminal remains on the surface (12). In this regard, the higher B_{max} value for the V53C-pyrene compared to that for the C-terminal peptide (Table 2) is likely due to a conformation in which some helices in a central part of the apoA-I molecule are out of contact with lipid leaving both the N- and C-terminal parts attached. Interestingly, a chaotropic perturbation study with GdnHCl suggested that HDL contains two populations of apoA-I in

which one is labile and readily dissociates while the other is strongly associated with HDL (55). In this regard, the recent finding that apoA-I adopts the extended belt conformation in both reconstituted discoidal and spherical HDL (56) is consistent with this conformation being that of the apoA-I strongly associated with spherical HDL particles. It is unclear how such an extended belt conformation of apoA-I on spherical HDL could interconvert to the helix bundle-closed conformation shown in this study.

A significant finding in this study is that the presence of cholesterol induces the helix bundle-open conformation of apoA-I bound to the SUV surface (Fig. 8). It is known that cholesterol in lipid membranes modulates the lipid interaction of apoA-I (42,43,46,48,57) or apoA-I mimetic peptides (58-60). Cholesterol has opposite effects on the acyl chain and headgroup regions in liquid-crystalline membranes (61): it decreases the fluidity of the acyl chain region and thereby reduces penetration of the amphipathic α-helices of the protein into the membranes (57,58,60), whereas it increases the separation of phospholipid headgroups and thereby facilitates the binding of apoA-I to lipid bilayers (43,46). Since the C-terminal helical region that has the strongest lipid affinity in the apoA-I molecule is expected to penetrate more deeply into the phospholipid membrane than the N-terminal helices (10), it is likely that the presence of cholesterol prevents the deep penetration of the C-terminal helices into the membrane (58), leading to alteration of the binding competition between the N- and C-terminal helices (12). As a result, apoA-I would tend to bind to the cholesterol-containing lipid surface in the helix bundle-open conformation in which both the N- and C-terminal helices are in contact with lipids. Indeed, it has been reported that the presence of cholesterol increases the binding affinity and decreases the number of apoA-I bound to SUV (46), supporting the idea that cholesterol induces the helix bundle-open conformation of apoA-I on the lipid surface. Such a conformational alteration when apoA-I interacts with the cholesterol-containing membranes appears to be relevant to the formation of nascent HDL particles via interaction of apoA-I with ABCA1 (7). Since the lipid binding affinity of apolipoprotein is critical for efficient membrane solubilization (62), the preferable binding of apoA-I with the helix bundle-open conformation to the vesiculated cholesterol-rich membranes would enhance the solubilization of membrane lipids, leading to the formation of nascent HDL particles.

In conclusion, the present study demonstrated that apoA-I has a flexible lipid-bound structure on spherical lipid particles, in which the N-terminal helix bundle adopts either open or closed conformations anchored by the C-terminal domain, depending upon the availability of space on the surface and the surface composition. The alterations in particle size and surface lipid composition such as cholesterol content of lipoproteins during remodeling in plasma would change the dynamic equilibrium between lipid-bound conformations of apoA-I, leading to the multiple functions of apoA-I. In addition, the concept of the variable lipid-bound conformation of apoA-I provides insight into the reaction process in which apoA-I binds to cell membranes via apoA-I/ABCA1 interaction to create nascent HDL particles.

Acknowledgements

The authors thank Drs. Saburo Aimoto and Toru Kawakami (Institute for Protein Research, Osaka University, Japan) for their help with ITC measurements.

This work was supported by NIH grant HL22633, Takeda Science Foundation, and Suzuken Memorial Foundation.

Abbreviations

ABC, ATP-binding cassette
apoA-I, apolipoprotein A-I
CD, circular dichroism
DMPC, dimyristoylphosphatidylcholine

5-DSA, 5-doxylstearic acid
GdnHCl, guanidine hydrochloride
HDL, high density lipoprotein
ITC, isothermal titration calorimetry
PC, phosphatidylcholine
SUV, small unilamellar vesicle
WT, wild type

REFERENCES

1. Castelli WP, Garrison RJ, Wilson PW, Abbott RD, Kalousdian S, Kannel WB. Incidence of coronary heart disease and lipoprotein cholesterol levels. The Framingham Study. J. Am. Med. Assoc 1986;256:2835–2838.
2. Movva R, Rader DJ. Laboratory assessment of HDL heterogeneity and function. Clin Chem 2008;54:788–800. [PubMed: 18375481]
3. Curtiss LK, Valenta DT, Hime NJ, Rye KA. What is so special about apolipoprotein AI in reverse cholesterol transport? Arterioscler Thromb Vasc Biol 2006;26:12–19. [PubMed: 16269660]
4. Rader DJ. Molecular regulation of HDL metabolism and function: implications for novel therapies. J Clin Invest 2006;116:3090–3100. [PubMed: 17143322]
5. Tall AR. Cholesterol efflux pathways and other potential mechanisms involved in the athero-protective effect of high density lipoproteins. J Intern Med 2008;263:256–273. [PubMed: 18271871]
6. Zannis VI, Chroni A, Krieger M. Role of apoA-I, ABCA1, LCAT, and SR-BI in the biogenesis of HDL. J Mol Med 2006;84:276–294. [PubMed: 16501936]
7. Vedhachalam C, Duong PT, Nickel M, Nguyen D, Dhanasekaran P, Saito H, Rothblat GH, Lund-Katz S, Phillips MC. Mechanism of ATP-binding cassette transporter A1-mediated cellular lipid efflux to apolipoprotein A-I and formation of high density lipoprotein particles. J Biol Chem 2007;282:25123–25130. [PubMed: 17604270]
8. Oram JF, Vaughan AM. ATP-Binding cassette cholesterol transporters and cardiovascular disease. Circ Res 2006;99:1031–1043. [PubMed: 17095732]
9. Segrest JP, Jones MK, De Loof H, Brouillette CG, Venkatachalapathi YV, Anantharamaiah GM. The amphipathic helix in the exchangeable apolipoproteins: a review of secondary structure and function. J. Lipid Res 1992;33:141–166. [PubMed: 1569369]
10. Palgunachari MN, Mishra VK, Lund-Katz S, Phillips MC, Adeyeye SO, Alluri S, Anantharamaiah GM, Segrest JP. Only the two end helixes of eight tandem amphipathic helical domains of human apo A-I have significant lipid affinity. Implications for HDL assembly. Arterioscler. Thromb. Vasc. Biol 1996;16:328–338. [PubMed: 8620350]
11. Saito H, Dhanasekaran P, Nguyen D, Deridder E, Holvoet P, Lund-Katz S, Phillips MC. α-Helix formation is required for high affinity binding of human apolipoprotein A-I to lipids. J. Biol. Chem 2004;279:20974–20981. [PubMed: 15020600]
12. Wang L, Hua N, Atkinson D, Small DM. The N-terminal (1-44) and C-terminal (198-243) peptides of apolipoprotein A-I behave differently at the triolein/water interface. Biochemistry 2007;46:12140–12151. [PubMed: 17915945]
13. Fang Y, Gursky O, Atkinson D. Structural studies of N- and C-terminally truncated human apolipoprotein A-I. Biochemistry 2003;42:6881–6890. [PubMed: 12779343]
14. Tanaka M, Dhanasekaran P, Nguyen D, Ohta S, Lund-Katz S, Phillips MC, Saito H. Contributions of the N- and C-terminal helical segments to the lipid-free structure and lipid interaction of apolipoprotein A-I. Biochemistry 2006;45:10351–10358. [PubMed: 16922511]
15. Saito H, Dhanasekaran P, Nguyen D, Holvoet P, Lund-Katz S, Phillips MC. Domain structure and lipid interaction in human apolipoproteins A-I and E, a general model. J. Biol. Chem 2003;278:23227–23232. [PubMed: 12709430]
16. Silva RA, Hilliard GM, Fang J, Macha S, Davidson WS. A three-dimensional molecular model of lipid-free apolipoprotein A-I determined by cross-linking/mass spectrometry and sequence threading. Biochemistry 2005;44:2759–2769. [PubMed: 15723520]

17. Ajees AA, Anantharamaiah GM, Mishra VK, Hussain MM, Murthy HM. Crystal structure of human apolipoprotein A-I: insights into its protective effect against cardiovascular diseases. Proc. Natl. Acad. Sci. U. S. A 2006;103:2126–2131. [PubMed: 16452169]
18. Saito H, Lund-Katz S, Phillips MC. Contributions of domain structure and lipid interaction to the functionality of exchangeable human apolipoproteins. Prog. Lipid Res 2004;43:350–380. [PubMed: 15234552]
19. Tanaka M, Koyama M, Dhanasekaran P, Nguyen D, Nickel M, Lund-Katz S, Saito H, Phillips MC. Influence of tertiary structure domain properties on the functionality of apolipoprotein A-I. Biochemistry 2008;47:2172–2180. [PubMed: 18205410]
20. Lund-Katz S, Liu L, Thuahnai ST, Phillips MC. High density lipoprotein structure. Front. Biosci 2003;8:d1044–1054. [PubMed: 12700101]
21. Davidson WS, Silva RA. Apolipoprotein structural organization in high density lipoproteins: belts, bundles, hinges and hairpins. Curr. Opin. Lipidol 2005;16:295–300. [PubMed: 15891390]
22. Thomas MJ, Bhat S, Sorci-Thomas MG. The use of chemical cross-linking and mass spectrometry to elucidate the tertiary conformation of lipid-bound apolipoprotein A-I. Curr Opin Lipidol 2006;17:214–220. [PubMed: 16680024]
23. Davidson WS, Thompson TB. The structure of apolipoprotein A-I in high density lipoproteins. J Biol Chem 2007;282:22249–22253. [PubMed: 17526499]
24. Martin DD, Budamagunta MS, Ryan RO, Voss JC, Oda MN. Apolipoprotein A-I assumes a “looped belt” conformation on reconstituted high density lipoprotein. J Biol Chem 2006;281:20418–20426. [PubMed: 16698792]
25. Wu Z, Wagner MA, Zheng L, Parks JS, Shy JM 3rd, Smith JD, Gogonea V, Hazen SL. The refined structure of nascent HDL reveals a key functional domain for particle maturation and dysfunction. Nat Struct Mol Biol 2007;14:861–868. [PubMed: 17676061]
26. Shih AY, Sligar SG, Schulten K. Molecular models need to be tested: the case of a solar flares discoidal HDL model. Biophys J 2008;94:L87–89. [PubMed: 18375520]
27. Narayanaswami V, Ryan RO. Molecular basis of exchangeable apolipoprotein function. Biochim. Biophys. Acta 2000;1483:15–36. [PubMed: 10601693]
28. Wang L, Atkinson D, Small DM. The interfacial properties of ApoA-I and an amphipathic alpha-helix consensus peptide of exchangeable apolipoproteins at the triolein/water interface. J Biol Chem 2005;280:4154–4165. [PubMed: 15695525]
29. Saito H, Dhanasekaran P, Baldwin F, Weisgraber KH, Lund-Katz S, Phillips MC. Lipid binding-induced conformational change in human apolipoprotein E. Evidence for two lipid-bound states on spherical particles. J. Biol. Chem 2001;276:40949–40954. [PubMed: 11533033]
30. Li HH, Lyles DS, Pan W, Alexander E, Thomas MJ, Sorci-Thomas MG. ApoA-I structure on discs and spheres. Variable helix registry and conformational states. J. Biol. Chem 2002;277:39093–39101. [PubMed: 12167653]
31. Thomas MJ, Bhat S, Sorci-Thomas MG. Three dimensional models of high density lipoprotein apoA-I:Implications for its assembly and function. J Lipid Res 2008;49:1875–1883. [PubMed: 18515783]
32. Curtiss LK, Bonnet DJ, Rye KA. The conformation of apolipoprotein A-I in high-density lipoproteins is influenced by core lipid composition and particle size: a surface plasmon resonance study. Biochemistry 2000;39:5712–5721. [PubMed: 10801321]
33. Sparks DL, Phillips MC, Lund-Katz S. The conformation of apolipoprotein A-I in discoidal and spherical recombinant high density lipoprotein particles. 13C NMR studies of lysine ionization behavior. J. Biol. Chem 1992;267:25830–25838. [PubMed: 1464597]
34. Catte A, Patterson JC, Bashtovyy D, Jones MK, Gu F, Li L, Rampioni A, Sengupta D, Vuorela T, Niemela P, Karttunen M, Marrink SJ, Vattulainen I, Segrest JP. Structure of spheroidal HDL particles revealed by combined atomistic and coarse-grained simulations. Biophys J 2008;94:2306–2319. [PubMed: 18065479]
35. Sahoo D, Narayanaswami V, Kay CM, Ryan RO. Fluorescence studies of exchangeable apolipoprotein-lipid interactions. Superficial association of apolipophorin III with lipoprotein surfaces. J Biol Chem 1998;273:1403–1408. [PubMed: 9430675]

36. Sahoo D, Narayanaswami V, Kay CM, Ryan RO. Pyrene excimer fluorescence: a spatially sensitive probe to monitor lipid-induced helical rearrangement of apolipophorin III. Biochemistry 2000;39:6594–6601. [PubMed: 10828977]
37. Drury J, Narayanaswami V. Examination of lipid-bound conformation of apolipoprotein E4 by pyrene excimer fluorescence. J Biol Chem 2005;280:14605–14610. [PubMed: 15708851]
38. Tamamizu-Kato S, Kosaraju MG, Kato H, Raussens V, Ruysschaert JM, Narayanaswami V. Calcium-triggered membrane interaction of the alpha-synuclein acidic tail. Biochemistry 2006;45:10947–10956. [PubMed: 16953580]
39. Sparks DL, Lund-Katz S, Phillips MC. The charge and structural stability of apolipoprotein A-I in discoidal and spherical recombinant high density lipoprotein particles. J. Biol. Chem 1992;267:25839–25847. [PubMed: 1464598]
40. Ladokhin AS, Jayasinghe S, White SH. How to measure and analyze tryptophan fluorescence in membranes properly, and why bother? Anal. Biochem 2000;285:235–245. [PubMed: 11017708]
41. Tricerri MA, Behling Agree AK, Sanchez SA, Jonas A. Characterization of apolipoprotein A-I structure using a cysteine-specific fluorescence probe. Biochemistry 2000;39:14682–14691. [PubMed: 11087425]
42. Derksen A, Gantz D, Small DM. Calorimetry of apolipoprotein-A1 binding to phosphatidylcholine-triolein-cholesterol emulsions. Biophys. J 1996;70:330–338. [PubMed: 8770209]
43. Saito H, Miyako Y, Handa T, Miyajima K. Effect of cholesterol on apolipoprotein A-I binding to lipid bilayers and emulsions. J. Lipid Res 1997;38:287–294. [PubMed: 9162748]
44. Tajima S, Yokoyama S, Yamamoto A. Effect of lipid particle size on association of apolipoproteins with lipid. J. Biol. Chem 1983;258:10073–10082. [PubMed: 6411702]
45. Saito H, Dhanasekaran P, Baldwin F, Weisgraber KH, Phillips MC, Lund-Katz S. Effects of polymorphism on the lipid interaction of human apolipoprotein E. J. Biol. Chem 2003;278:40723–40729. [PubMed: 12917433]
46. Arnulphi C, Jin L, Tricerri MA, Jonas A. Enthalpy-driven apolipoprotein A-I and lipid bilayer interaction indicating protein penetration upon lipid binding. Biochemistry 2004;43:12258–12264. [PubMed: 15379564]
47. Tricerri MA, Sanchez SA, Arnulphi C, Durbin DM, Gratton E, Jonas A. Interaction of apolipoprotein A-I in three different conformations with palmitoyl oleoyl phosphatidylcholine vesicles. J Lipid Res 2002;43:187–197. [PubMed: 11861660]
48. Massey JB, Pownall HJ. Cholesterol is a determinant of the structures of discoidal high density lipoproteins formed by the solubilization of phospholipid membranes by apolipoprotein A-I. Biochim Biophys Acta 2008;1781:245–253. [PubMed: 18406360]
49. Okuhira K, Tsujita M, Yamauchi Y, Abe-Dohmae S, Kato K, Handa T, Yokoyama S. Potential involvement of dissociated apoA-I in the ABCA1-dependent cellular lipid release by HDL. J Lipid Res 2004;45:645–652. [PubMed: 14729855]
50. Pownall HJ, Ehnholm C. The unique role of apolipoprotein A-I in HDL remodeling and metabolism. Curr Opin Lipidol 2006;17:209–213. [PubMed: 16680023]
51. Rye KA, Barter PJ. Formation and metabolism of prebeta-migrating, lipid-poor apolipoprotein A-I. Arterioscler Thromb Vasc Biol 2004;24:421–428. [PubMed: 14592845]
52. Gursky O, Atkinson D. Thermal unfolding of human high-density apolipoprotein A-1: implications for a lipid-free molten globular state. Proc. Natl. Acad. Sci. USA 1996;93:2991–2995. [PubMed: 8610156]
53. Marcel YL, Kiss RS. Structure-function relationships of apolipoprotein A-I: a flexible protein with dynamic lipid associations. Curr. Opin. Lipidol 2003;14:151–157. [PubMed: 12642783]
54. Brouillette CG, Anantharamaiah GM. Structural models of human apolipoprotein A-I. Biochim. Biophys. Acta 1995;1256:103–129. [PubMed: 7766689]
55. Pownall HJ, Hosken BD, Gillard BK, Higgins CL, Lin HY, Massey JB. Speciation of human plasma high-density lipoprotein (HDL): HDL stability and apolipoprotein A-I partitioning. Biochemistry 2007;46:7449–7459. [PubMed: 17530866]
56. Silva RA, Huang R, Morris J, Fang J, Gracheva EO, Ren G, Kontush A, Jerome WG, Rye KA, Davidson WS. Structure of apolipoprotein A-I in spherical high density lipoproteins of different sizes. Proc Natl Acad Sci U S A 2008;105:12176–12181. [PubMed: 18719128]

57. Lecompte MF, Bras AC, Dousset N, Portas I, Salvayre R, Ayrault-Jarrier M. Binding steps of apolipoprotein A-I with phospholipid monolayers: adsorption and penetration. Biochemistry 1998;37:16165–16171. [PubMed: 9819208]

58. Egashira M, Gorbenko G, Tanaka M, Saito H, Molotkovsky J, Nakano M, Handa T. Cholesterol modulates interaction between an amphipathic class A peptide, Ac-18A-NH2, and phosphatidylcholine bilayers. Biochemistry 2002;41:4165–4172. [PubMed: 11900560]

59. Epand RM, Epand RF, Sayer BG, Datta G, Chaddha M, Anantharamaiah GM. Two homologous apolipoprotein AI mimetic peptides. Relationship between membrane interactions and biological activity. J Biol Chem 2004;279:51404–51414. [PubMed: 15358763]

60. Epand RM, Epand RF, Sayer BG, Melacini G, Palgulachari MN, Segrest JP, Anantharamaiah GM. An apolipoprotein AI mimetic peptide: membrane interactions and the role of cholesterol. Biochemistry 2004;43:5073–5083. [PubMed: 15109266]

61. Maxfield FR, Tabas I. Role of cholesterol and lipid organization in disease. Nature 2005;438:612–621. [PubMed: 16319881]

62. Gillotte KL, Zaiou M, Lund-Katz S, Anantharamaiah GM, Holvoet P, Dhoest A, Palgunachari MN, Segrest JP, Weisgraber KH, Rothblat GH, Phillips MC. Apolipoprotein-mediated plasma membrane microsolubilization. Role of lipid affinity and membrane penetration in the efflux of cellular cholesterol and phospholipid. J. Biol. Chem 1999;274:2021–2028. [PubMed: 9890960]

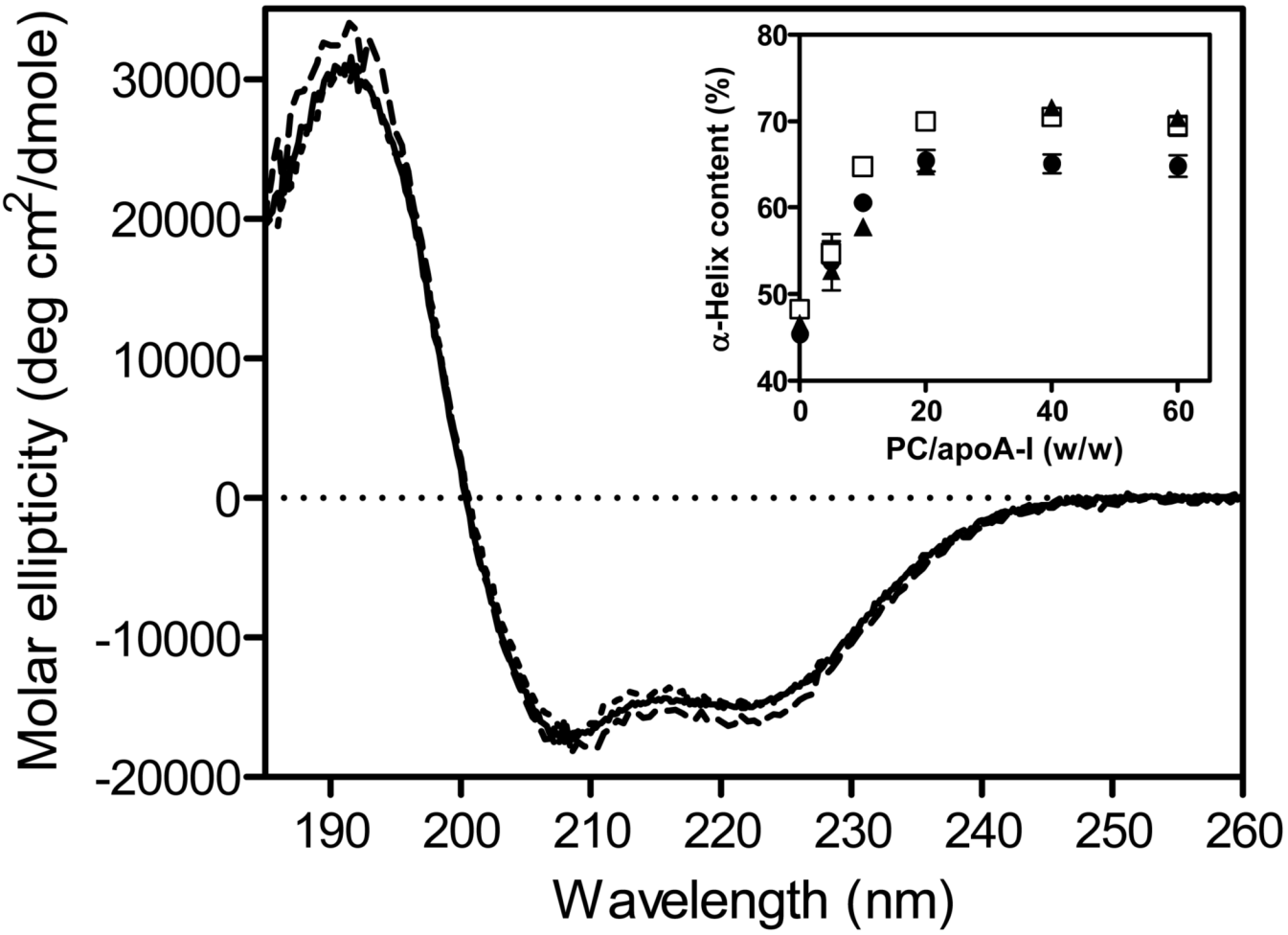

Fig. 1. Far-UV CD spectra of WT (solid line), V53C-pyrene (dashed line), and F229C-pyrene (dotted line) apoA-I in the lipid-free state

The *inset* shows the increase in α-helix content of the apoA-I variants bound to egg PC SUV as a function of the weight ratio of PC to apoA-I. ▲, WT apoA-I; □, apoA-I V53C-pyrene; • apoA-I F229C-pyrene. Protein concentration was 50 μg/ml.

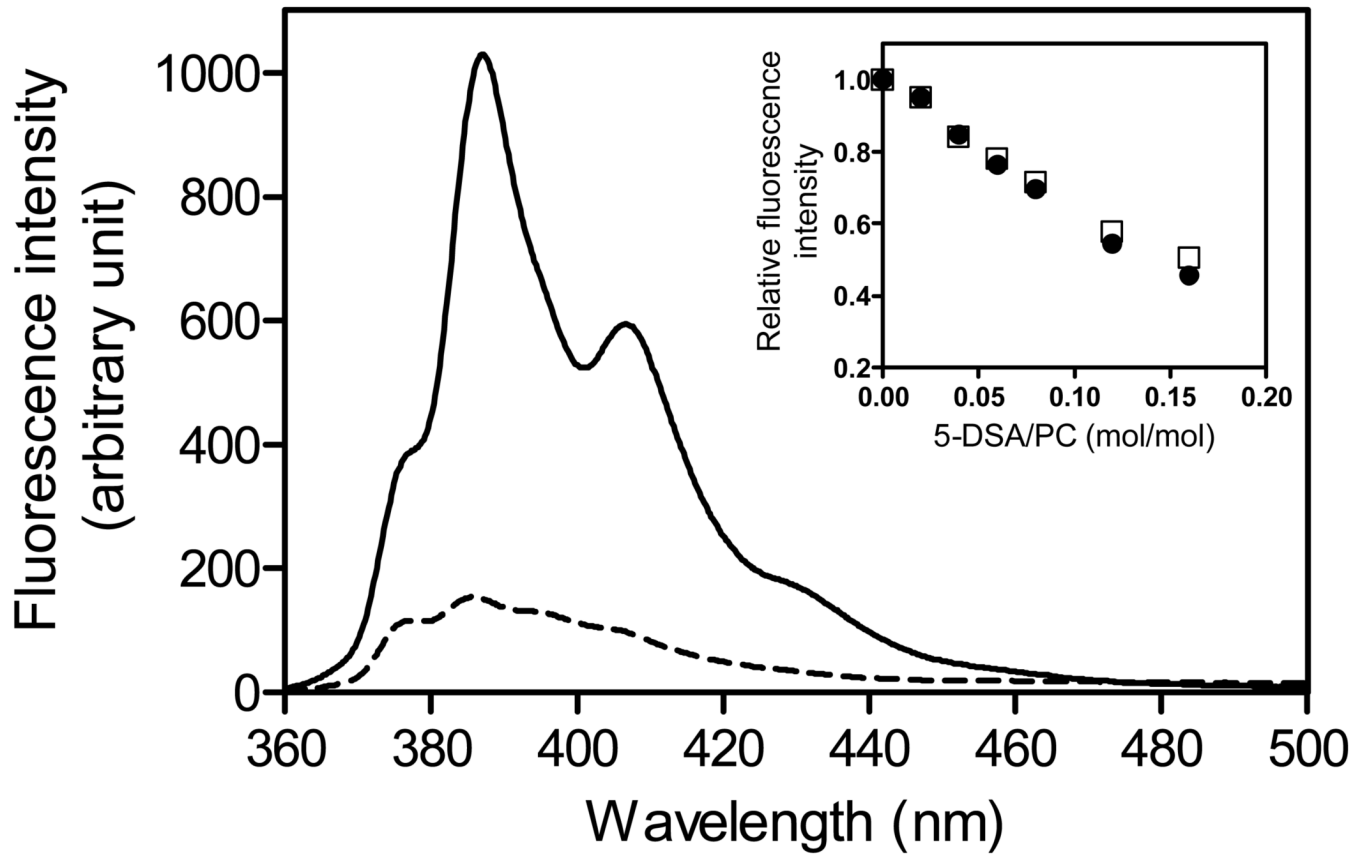

Fig. 2. Fluorescence emission spectra of pyrene-labeled apoA-I V53C mutant in the lipid-free (dashed line) or bound to egg PC SUV (solid line)

Protein and PC concentrations were 25 μg/ml and 1.0 mg/ml, respectively. The *inset* shows the relative changes in fluorescence of apoA-I V53C-pyrene (□) and F229C-pyrene (•) as a function of the molar ratio of 5-DSA to PC.

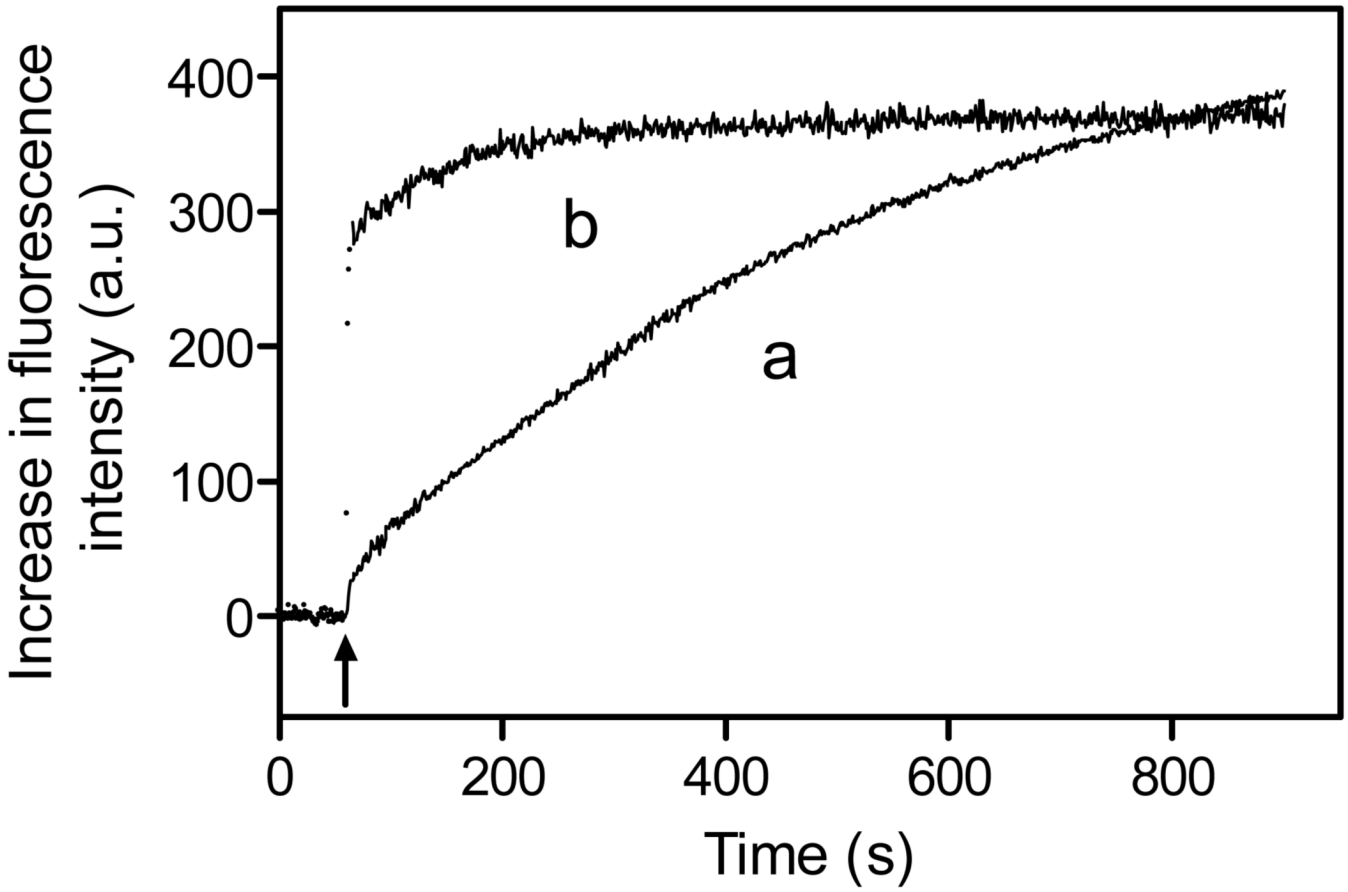

Fig. 3. Time courses of increases in fluorescence intensity upon addition of egg PC SUV to apoA-I V53C-pyrene (*trace a*) and F229C-pyrene (*trace b*)

SUV was added to apoA-I variants at final concentrations of 25 μg/ml protein and 1.0 mg/ml PC. Pyrene fluorescence was monitored at 385 nm with an excitation of 342 nm.

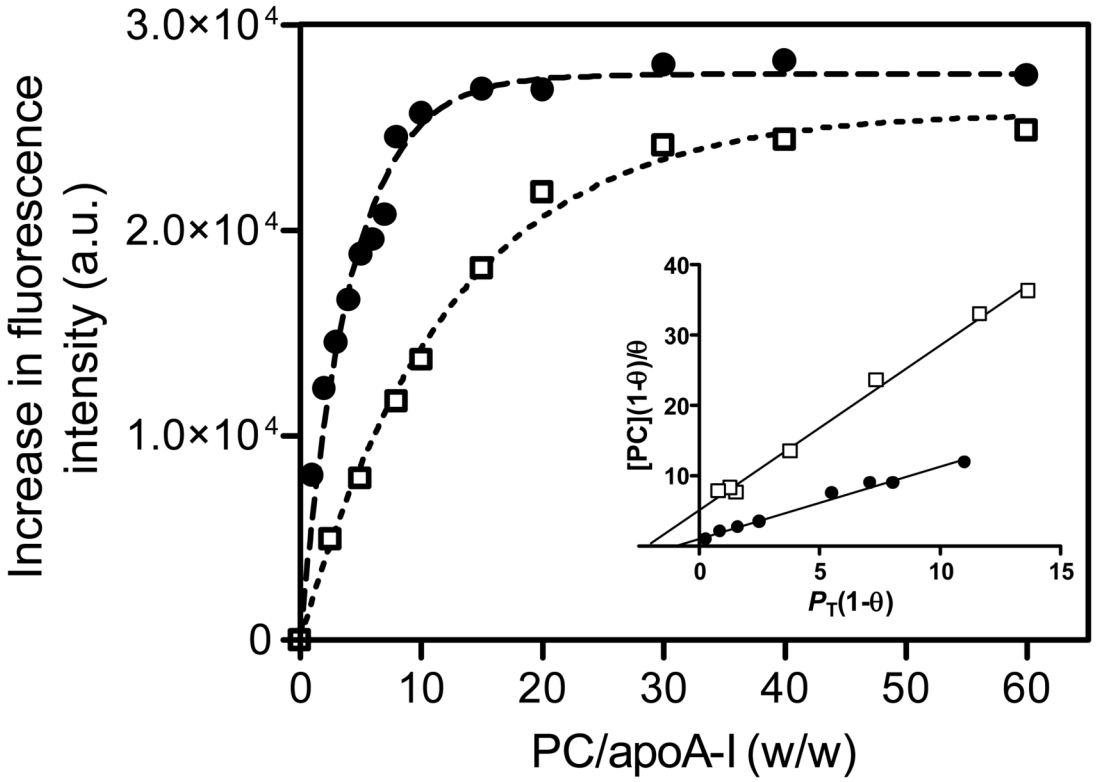

Fig. 4. Increase in fluorescence intensity of apoA-I V53C-pyrene (□) and F229C-pyrene (•) as a function of the weight ratio of PC to apoA-I

Protein concentration was 25 μg/ml. The *inset* shows the linearized plots using Equation 4.

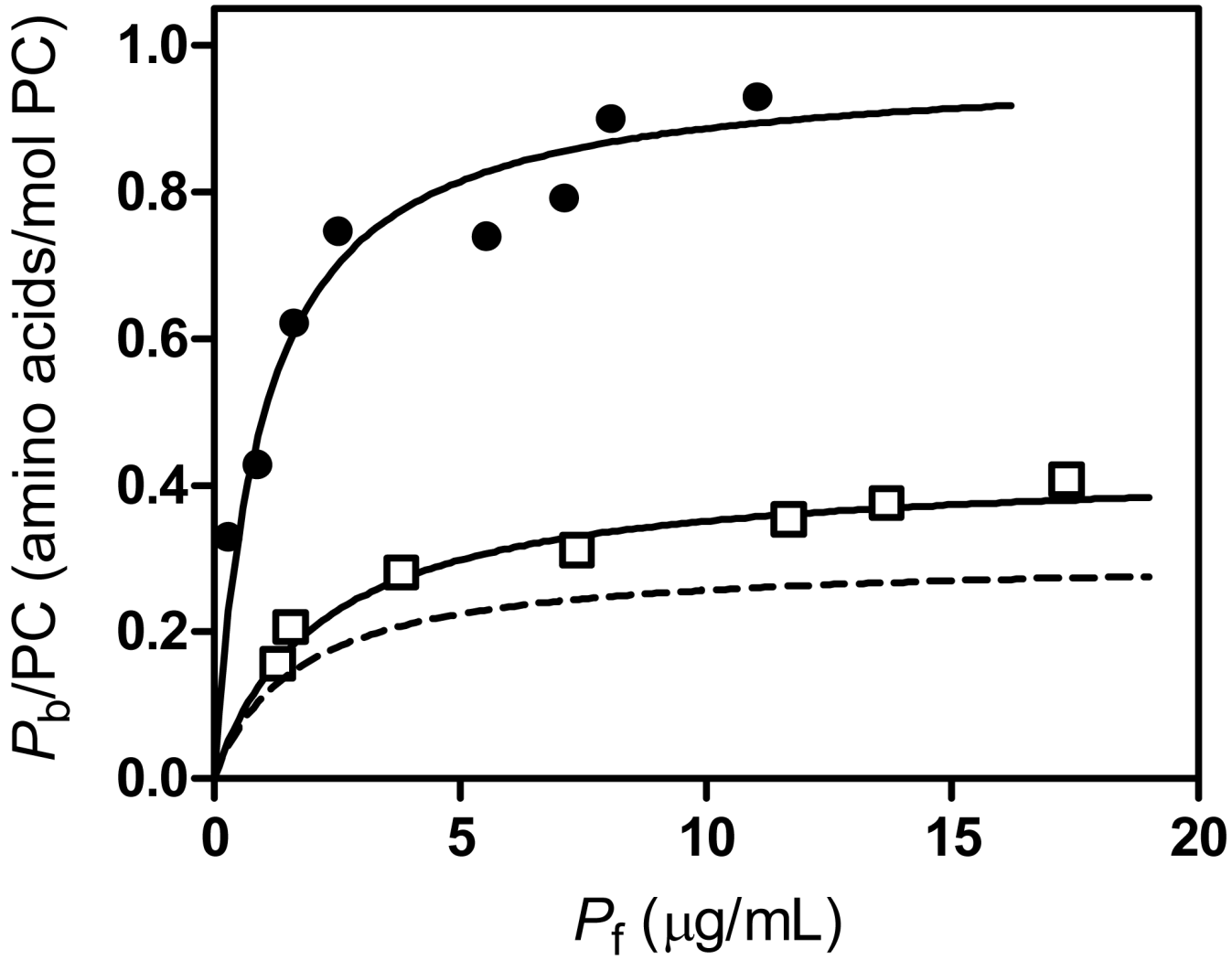

Fig. 5. Binding isotherms of apoA-I V53C-pyrene (□) and F229C-pyrene (•)
The solid lines are the theoretical binding isotherms calculated using Equation 2 and the parameters shown in Table 2. The binding isotherm for WT apoA-I obtained from gel filtration experiments is also shown (dashed line) for comparison (ref. 11).

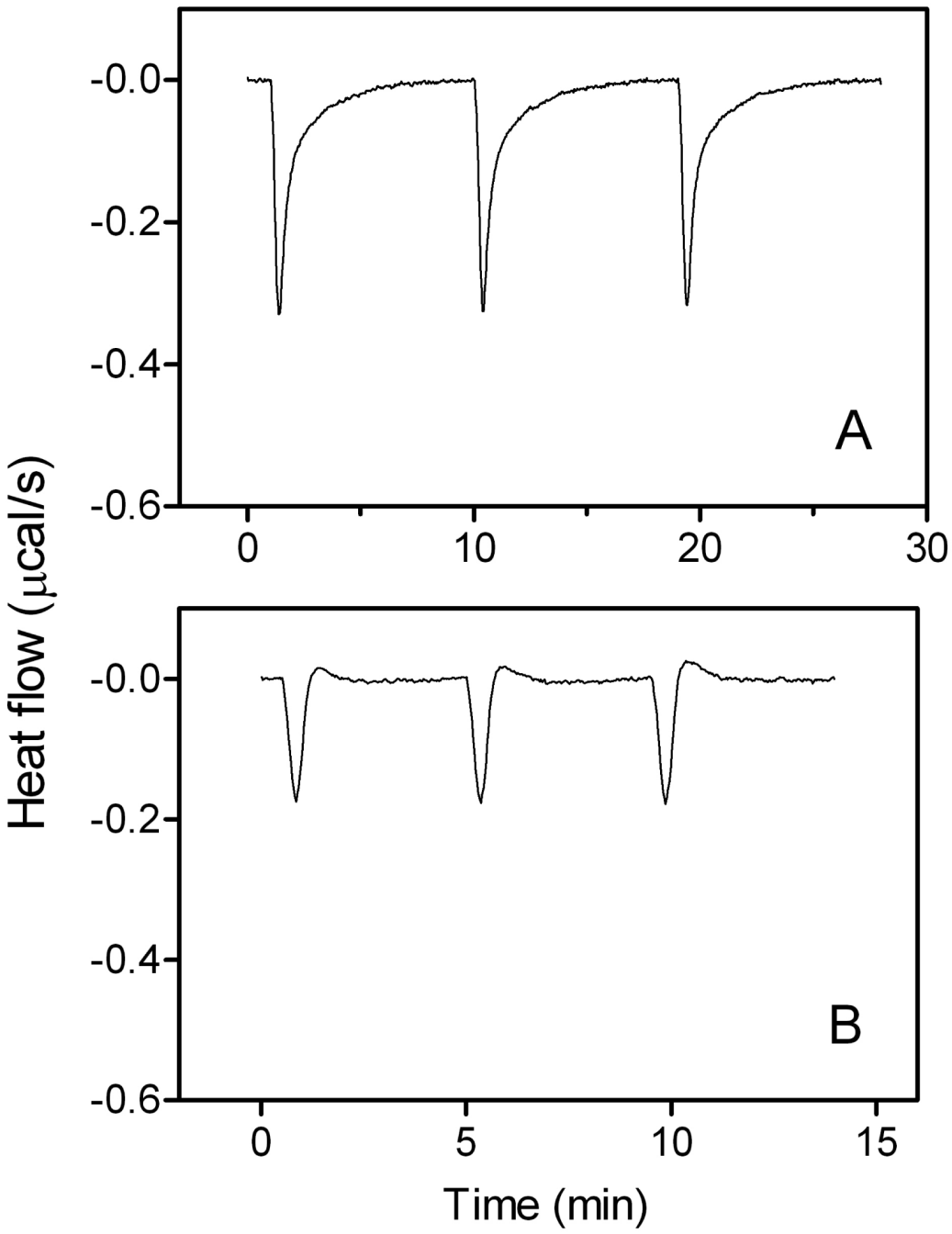

Fig. 6. Isothermal titration curves for binding of WT apoA-I to egg PC SUV

A, 8-μl aliquots of apoA-I solution (0.8 mg/ml) were injected into SUV (PC concentration of 15 mM). *B*, 10-μl aliquots of SUV (PC concentration of 15 mM) were injected into apoA-I solution (0.3 mg/ml).

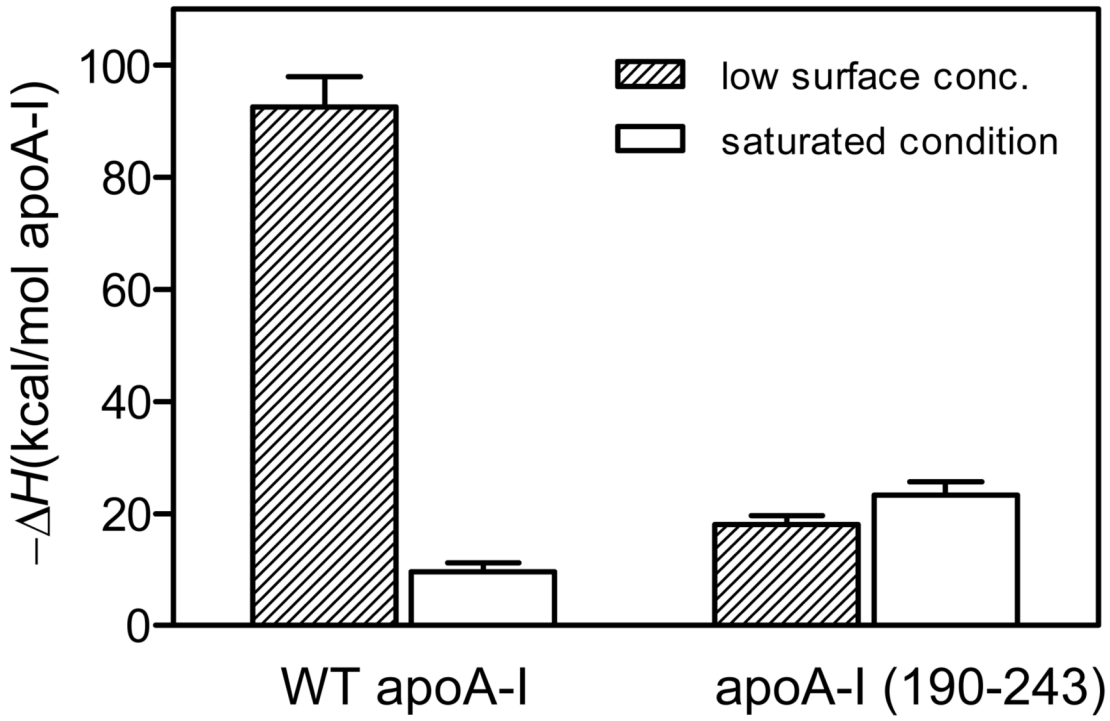

Fig. 7. Binding enthalpies of apoA-I WT and 190-243 fragment to egg PC SUV obtained under two limiting conditions

Protein solutions were injected into excess SUV at a PC-to-protein molar ratio of > 10,000 (low surface concentration) or SUV was injected into excess protein at a PC-to-protein molar ratio of < 10 (saturated condition).

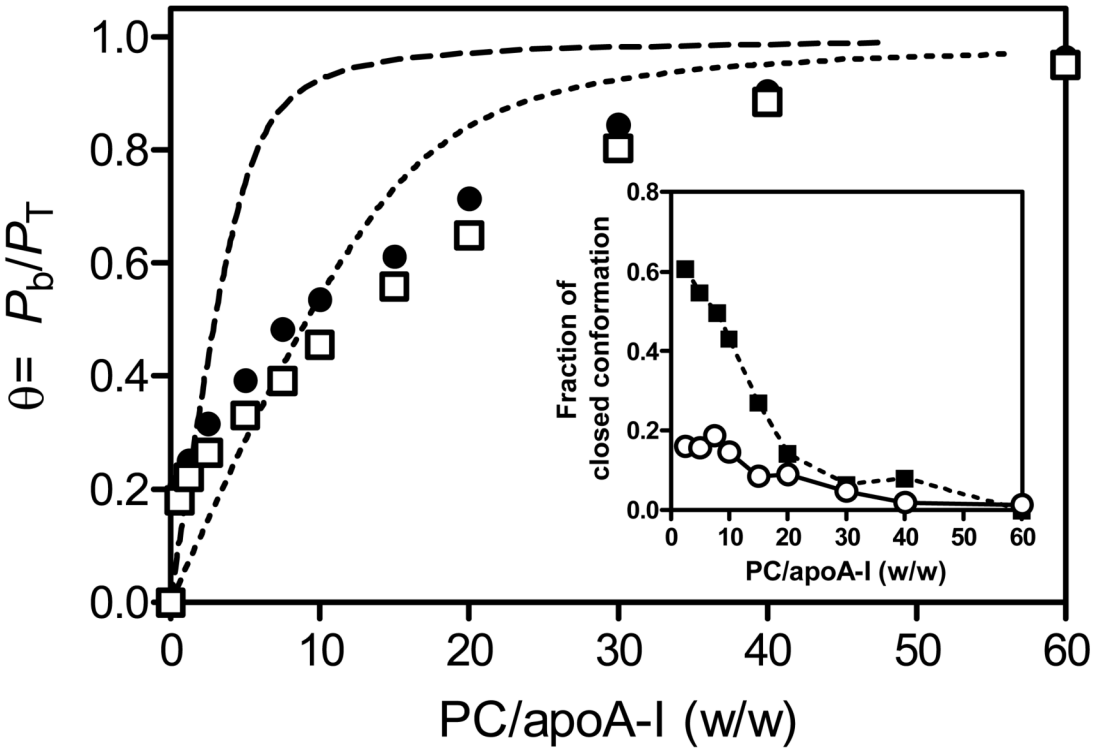

Fig. 8. Increase in fluorescence intensity of apoA-I V53C-pyrene (□) and F229C-pyrene (•) upon binding to egg PC/cholesterol (17/3 mol/mol) SUV

Protein concentration was 25 μg/ml. The titration curves for binding of V53C-pyrene (dotted line) and F229C-pyrene (dashed line) to egg PC SUV are also shown for comparison. The *inset* shows the effect of cholesterol on the change in the fraction of closed conformation of the helix bundle in apoA-I bound to SUV. ■, egg PC SUV; ▪, egg PC/cholesterol (17/3) SUV.

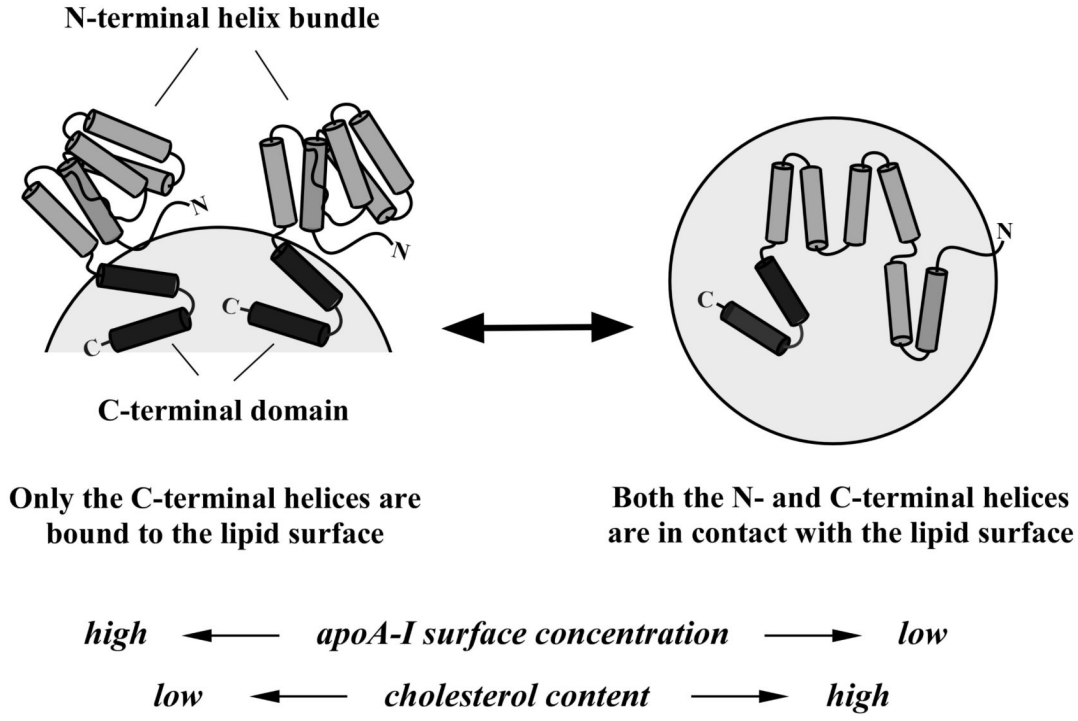

Fig. 9. Model of two possible conformations of apoA-I at the surface of a spherical lipid particle

At high apoA-I surface concentration, the N-terminal helix bundle remains closed and out of contact with the lipid surface (*left*). At low surface coverage where a greater surface area is available, the helix bundle is open so that the α-helices can make contact with the lipid surface (*right*). Cholesterol content in the lipid surface also modulates the equilibrium between the two conformations.

Table 1

Parameters for KI quenching of pyrene fluorescence of apoA-I variants

	lipid-free		SUV-bound	
apoA-I variants	f_a	K_{SV}	f_a	K_{SV}
		M^{-1}		M^{-1}
apoA-I V53C-pyrene	0.63 ± 0.02	5.5 ± 0.2	0.51 ± 0.02	5.9 ± 0.3
apoA-I F229C-pyrene	0.62 ± 0.02	11.7 ± 0.8	0.62 ± 0.02	9.0 ± 0.6

Table 2

Parameters for binding of apoA-I variants or peptides to egg PC SUV

apoA-I variants	K_d	B_{max}
	μg/ml	*amino acids/mol PC*
apoA-I V53C-pyrene	2.2 ± 0.3	0.43 ± 0.02
apoA-I F229C-pyrene	1.0 ± 0.3	0.97 ± 0.05
apoA-I 220-241/F229C-pyrene	4.9 ± 0.9	0.27 ± 0.02
WT apoA-I[a]	1.7 ±0.4	0.30 ± 0.02

[a]Values are from gel filtration experiments (ref.11)